

Received: 03 November 2020 / Accepted: 12 December 2020 / Published online: 29 March 2021

*tool wear, aerospace alloys,  
oxidation mechanism,  
diffusion couple method*

Wit GRZESIK<sup>1</sup>

## **INVESTIGATION OF NOTCH WEAR MECHANISMS IN THE MACHINING OF NICKEL-BASED INCONEL 718 ALLOY**

This paper highlights tool wear mechanisms in the machining of heat resistance alloys including nickel-based Inconel 718 alloy which is one of the most popular material in the aircraft industry. Special attention was paid to the notch wear which develops on the flank face due to high temperature oxidation of the cutting tool material at temperature of about 800°C. The experimental procedure includes the diffusion couple methods and tool wear tests which assess the degradation of the deposited coating. The obtained results were supported by SEM images of the flank face periphery and EDS analysis performed in the regions of intensive oxidation. Some conclusions and ongoing research on the investigation of the oxidation phenomenon of cutting tool materials are outlined.

### **1. INTRODUCTION**

Wider application of advanced construction materials with special functional properties in many industrial sectors exerts a strong pressure on cutting tool manufactures to develop new coated cutting tool materials which can withstand extremely high temperature and contact pressure occurring. For instance in aerospace industry the most popular materials are Ni-based Inconel 718 and Ti-based Ti6Al4V alloys [1, 2]. Some important properties which can be featured by cutting tools in use include high hot hardness, high chemical affinity and superior resistance to oxidation which occurs due to penetration of atmospheric air to the cutting zone in dry machining [1, 3]. In particular,  $Ti_{1-x}Al_xN$  and  $Al_xTi_{1-x}N$  coatings with different stoichiometry ratio Al/Ti ( $x = 0.5-0.7$ ) are applied in the limited machining operations of Ti-based and Ni-based heat resistant superalloys (HRSA) [2, 3]. It was documented that high Al content in the TiAlN (AlTiN) coating promotes the formation of outer  $Al_2O_3$  layer during machining operations in which cutting temperature increases to about 800°C. The problem is that the higher Al content reduces the oxidation rate and the tool protection is not sufficient [4]. The same level of cutting temperature, i.e. above 800°C was determined using 3D FEM simulation with the cutting speed of 80 m/min, feed rate of  $f = 0.1$  mm/rev and depth of cut of 0.25 mm [5].

---

<sup>1</sup> Manufacturing and Materials Engineering, Opole University of Technology, Opole, Poland

\* E-mail: w.grzesik@po.edu.pl

<https://doi.org/10.36897/jme/131821>

However, under high cutting temperature the coating material is subjected to atmospheric oxygen causing so-called notch wear which results in formation of a groove at the distance equal to the depth of cut [1, 6, 7]. Tool wear mechanisms when machining Inconel 718 alloy using specially tailored TiAlN coated inserts were investigated in own research studies [8]. They confirmed the predominant appearance of notch wear mechanism on the flank face in dry machining of this superalloy. Similar study focuses on the chemical and diffusional interactions between superalloy Inconel 718 and cubic boron nitride (cBN) tool material is reported in ref. [9]. It covers thermodynamic modeling and experimental tests in the pressure range of 0.1 Pa to 2.5 GPa at temperatures up to 1600°C. The methods used include diffusion couples under both vacuum and high pressure, transmission electron microscopy (TEM) analysis and in-situ synchrotron observations.

Consequently, a real research problem appears how to predict the formation of Al<sub>2</sub>O<sub>3</sub> protective layer for machining applications. At present, some diffusion tests, for instance diffusion couple tests, performed in vacuum or in air are proposed to replicate notch wear conditions by varying the time and oxidation temperature [10, 11]. Recently, X-ray photoelectron spectroscopy was used to study the evolution of surface chemistry and to reconstruct elemental distribution profiles [12]. It was revealed that the Ti<sub>1-x</sub>Al<sub>x</sub>N oxidation scenario depends on both  $x$  ratio and the annealing temperature ( $T_a$ ).

In this study a series of oxidation tests were performed under the constant temperature of 900°C and variable annealing time using the diffusion couple method. The oxidation occurs at the interface between using TiAlN PVD-coating and a special Inconel 718 (IN 718) coupon. Previously, the experimental study on the application of diffusion couple method to detect the oxidation process between TiAlN coating and Inconel 718 was presented in Ref. [13]. The obtained data were compared with tool wear tests under dry machining conditions and different machining times. It was reasoned that oxidation effects documented by XRD and EDS analysis of the oxidized coating surfaces are similar for the static diffusion-couples and dynamic tool wear tests.

## 2. CHARACTERIZATION OF TOOL AND WORKPIECE MATERIALS

### 2.1. CUTTING TOOL AND WORKPIECE MATERIALS

Cutting tools coated with PVD TiAlN (atomic ratio Ti:Al of 0.45:0.55 -Ti<sub>0.45</sub>Al<sub>0.55</sub>N) layer with the coating thickness of about 3 μm were selected. They were commercial rhombic shaped cutting inserts of a KC5010 grade by Kennametal.

The following chemical compositions of the TiAlN coating were detected by EDS analysis performed before oxidation process: 27.08 at.% Ti, 21.39 at.% Al, 51.53 at.% N.

In this experimental study, heat-resistant aerospace superalloy (HRSA) Ni-based grade Inconel (IN) 718 (PWA 1469-4 commercial grade with surface hardness around 36 HRC), was used as workpiece material. In the aerospace industry Inconel 718 is frequently used to made highly thermally loaded parts of turbo engines, such as blades and cases [8]. The following chemical composition of the Inconel 718 nickel-based alloy was detected by

EDS analysis – 54.93 at.% Ni, 21.06 at.% Cr, 16.53 at.% Fe, 3.31 at.% Nb, 2.93 at.% Mo, 1.05 at.% Ti and 0.35 at.% Mn. On the other hand, Table 1 specifies the chemical composition (wt%) of the IN 718 used.

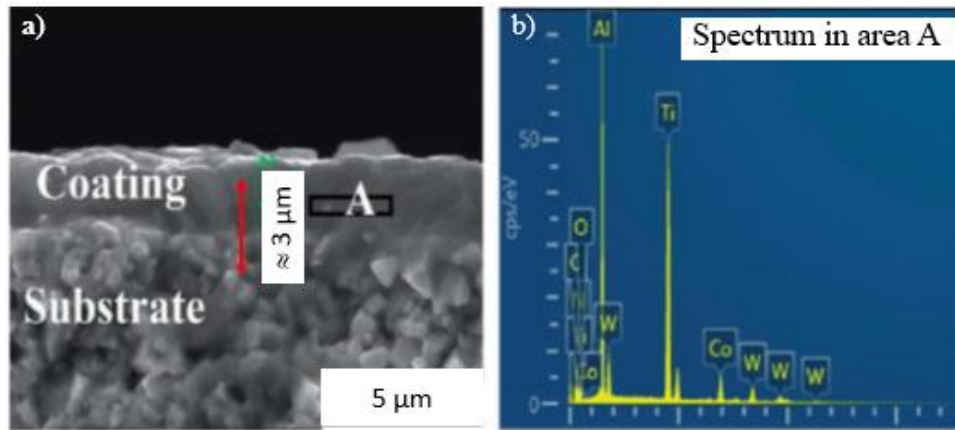


Fig. 1. TiAlN coating deposited on WC-Co substrate: (a) cross-sectional SEM image and (b) result of EDS analysis in area A [13, 14 ]

Table 1. Specified chemical composition (wt%) of Inconel 718 alloy with Ni as balance

Cr	Co	Fe	C	Mo	Al	Ti	Nb
18.4	0.3	17.5	0.04	3.0	0.6	0.9	5.5

## 2.2. OXIDATION TESTS USING DIFFUSION COUPLE METHOD

The oxidation tests were performed in a controlled atmosphere furnace equipped with a precision temperature sensor. The diffusion couples consisting of TiAlN coated inserts and special coupons (see Fig. 1) made of Inconel 718 alloy in the form of 2 mm thick plates were annealed at the constant temperature of 900°C during variable time of 2.5, 10 and 30 min [13].

The oxidation effect was assessed by measurements of the mass before and after annealing using a precision weighting with the resolution of  $\pm 0.1$  mg [13]. As a result, the mass of the deposited top  $\text{Al}_2\text{O}_3$  layer by area unit ( $m_{ol}$ ) was determined and its thickness ( $t_{ol}$ ) was assessed from Eq. (1), i.e.

$$t_{ol} = \frac{\Delta m_{ol}}{\rho A_u} \quad (1)$$

where:  $\Delta m_{ol}$  is the mass increment in  $\text{mg}/\text{cm}^2$ ,  $\rho$  is the density of  $\text{Al}_2\text{O}_3$  equal to  $3986 \text{ kg}/\text{m}^3$  and  $A_u$  is the unit area in  $\text{cm}^2$ .

The static diffusion couple method was applied in order to quantify the diffusion interactions between the TiAlN coating and Inconel 718 samples in the form of a thin disc of about 2 mm in thickness. The contact disc surfaces were polished to a mirror finish using ultra fine abrasives and ultrasonically cleaned in isopropanol. Moreover, the couples were

pressed by a mass of 15 kg to promote strong contact and intensify chemical reactivity at high temperatures. As previously, the coating and coupon surfaces were examined in terms of oxidation effects. Scanning electron microscopy was performed on a JEOL 840A microscope equipped with an Oxford EDX detector. X-ray studies of the oxidation layers formed in all tests were performed in X'Pert PRO PANalytical machine using filtered radiation of a lamp with the cobalt anode.

Fig. 2 presents the setup of diffusion couple test in which the commercial cutting tool insert (1) is coupled with a disc-shaped material (2) (Fig. 2a). As a result, the diffusion at the couple interface develops correspondingly to the contact conditions created by the normal load of 150 N on the flank face.

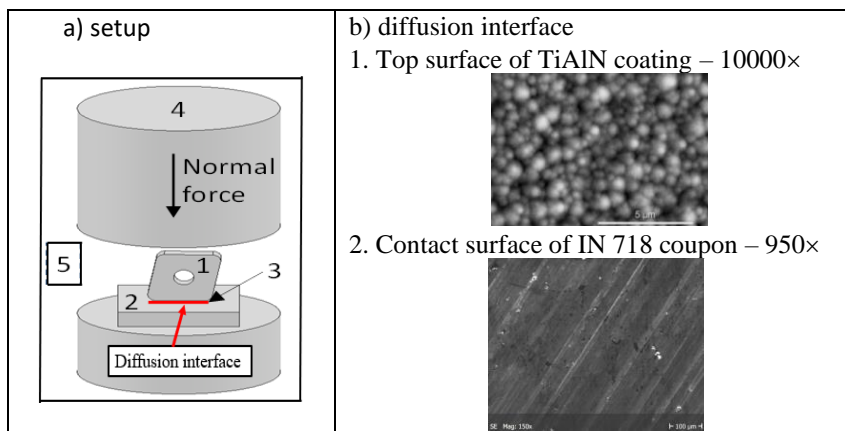


Fig. 2. Schematic setup of static diffusion couple test (a) and contact surfaces of the diffusion couple (b) 1- cutting insert, 2 - IN 718 coupon, 3- diffusion bond, 4- ceramic mass, 5- furnace with flowing oxygen [13]

### 2.3. CUTTING PARAMETERS AND TOOL WEAR TESTS

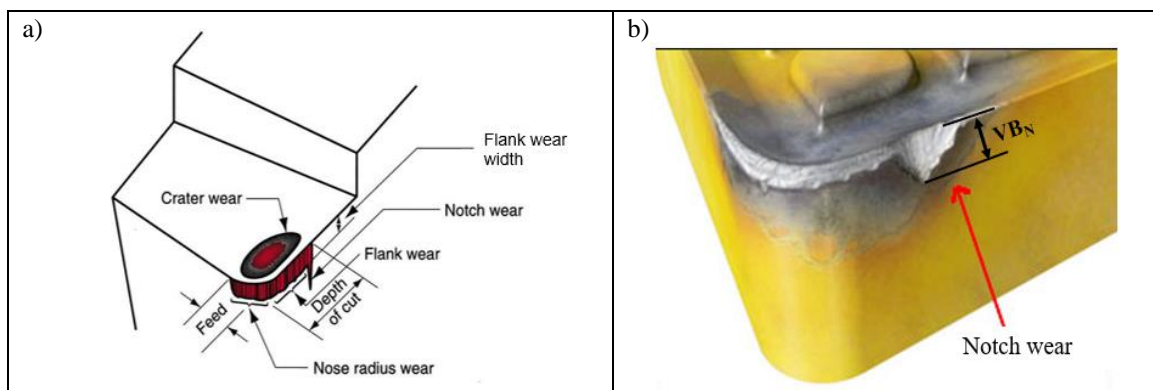


Fig. 3. Image of a worn cutting tool showing the principal locations and characteristic wear types (a) and worn cutting inserts with developed notch wear at the primary cutting edge (b)

In this investigation the cutting speed of 200 m/min, the depth of cut of  $a_p = 0.25$  mm and the feed rate of  $f = 0.1$  mm/rev were selected for turning operations of Inconel 718 bars. Two short machining trials during 0.5 and 2 min were carried out in order to expose

the oxidized  $\text{Al}_2\text{O}_3$  layer on the rake and flank faces and to show the development of notch wear ( $VB_N$ ), which is predominantly caused by ambient air penetrating from the periphery of the flank face [1, 5]. The visualized and real wear scars observed on the cutting tool are presented in Fig. 3.

### 3. EXPERIMENTAL RESULTS AND DISCUSSION

#### 3.1. QUANTIFICATION OF OXIDATION PROCESS

##### 3.1.1. MASS AND THICKNESS VARIATION DURING OXIDATION PROCESS

As mentioned in Section 2.2 the mass of oxidized layers produced during annealing performed at  $900^\circ\text{C}$  during 2.5, 10 and 30 min was measured. The measured values of mass increment resulting from coating oxidation are presented in Fig. 4a. It is evident that the masses of oxidized layers deposited on TiAlN coating in the diffusion couple by contact with Inconel 718 increase visibly depending on the annealing time. In particular, as shown in Fig. 4a, the increase in the annealing time from 2.5 min to 30 min causes that the mass of oxidized layer ( $m_{ol}$ ) increases from 0.2 to  $1.4 \text{ mg/cm}^2$ . That means the mass increment per area unit (oxidation rate) ( $\Delta m_{ol}$ ) depends predominantly on the oxidation duration of the diffusion interface.

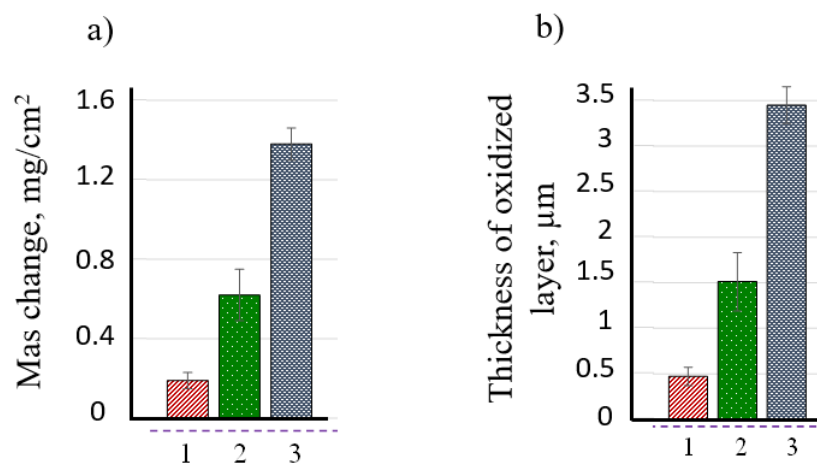


Fig. 4. The mass (a) and thickness (b) changes of investigated samples oxidized at the temperature of  $900^\circ\text{C}$  for the annealing time of 2.5 min (1), 10 min (2) and 30 min (3)

The annealing time influences the oxidation effects in such a way that for the mass increased by about 300% and 200% when the annealing was continued from the shortest time of 2.5 min up to 10 and 30 min respectively. The corresponding values of the thicknesses of oxidized layers calculated using Eq. (1) are presented in Fig. 4a. It can be concluded based on the estimations presented in Fig. 4b that the thickness of the oxidized layer increases by

about three times (from about 0.5  $\mu\text{m}$  to about 1.5  $\mu\text{m}$ ) when the annealing time increases from 2.5 min to 10 min. After 30 min the thickness ( $t_{ol}$ ) increases above 3  $\mu\text{m}$ , so the coating is probably fully oxidized. It can be noted that for the annealing during 5 min, the oxidized layer thickness can be expected to reach the level of 1  $\mu\text{m}$ . In general, the empirical models of mass and thickness vs. annealing time shown in Figs. 4a and 4b satisfy the exponential function.

### 3.1.2. CHANGES OF CHEMICAL COMPOSITION OF COUPLED SURFACES DURING OXIDATION PROCESS

Appropriate changes of four main chemical components (Ti, Al, N and O in at.%) and additional components Ni and Cr which diffused from the IN 718 coupon to the TiAlN coating determined by means of EDS analysis are specified in Table 2 and presented graphically in Fig. 5. It was documented in the previous study [13] that the onset of oxidation can be observed at 700°C but the  $\text{Al}_2\text{O}_3$  layer of about 2  $\mu\text{m}$  thickness can be formed on the TiAlN coating at higher temperatures of about 900°C and annealing time of about 15 min which agrees with data in Ref. [5]. As reported in Ref. [12], a double-layer oxide ( $\text{Al}_2\text{O}_3/\text{TiO}_2$ ) can be formed for  $\text{Ti}_{0.55}\text{Al}_{0.45}\text{N}$  coating but after 1 h annealing in dry air at  $T_a = 500^\circ\text{C}$ .

Table 2. The estimated chemical composition of surface layer (measured by EDS) for TiAlN + IN 718 samples oxidized at temperature 900°C for 2.5, 10 and 30 min

Element (at%)/ Time	2.5	10	30
O	17.12	18.81	20.31
Al	23.11	22.98	22.12
N	35.22	33.75	31.29
Ti	12.21	11.96	11.08
Ni	7.03	7.50	10.17
Cr	5.31	5.00	5.03

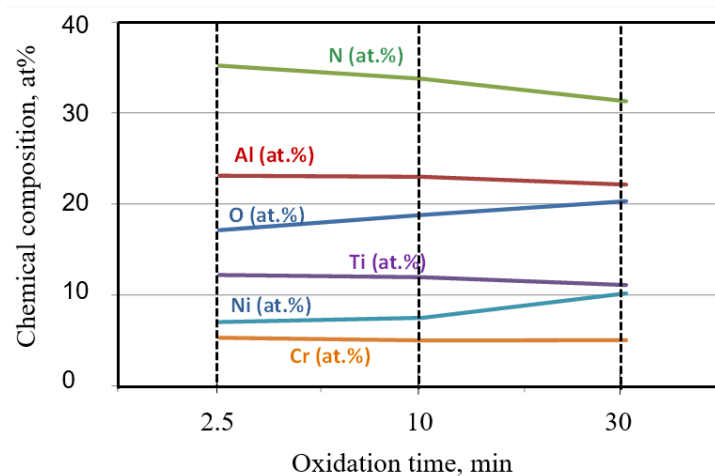


Fig. 5. Changes of chemical elements at the temperature of 900°C for the annealing time of 2.5 min, 10 min and 30 min

Figure 5 depicts that N content of about 33at% (as average value) detected after oxidation is distinctly lower than in the initial state (51.53at%). Al content remains practically the same at the level of about 22at%. At the same time, the Ti content drastically decreases from about 27at% down to about 12at% independently of the annealing time. The presence of Cr (about 5at%) and Ni (about 8at%) suggests that both these elements diffused to the TiAlN coatings during its oxidization from the coupled IN 718 sample.

### 3.1.3. OXIDATION PRODUCT CHARACTERIZATION USING XRD ANALYSIS

It was observed based on the changes of chemical composition of  $\text{Al}_2\text{O}_3$  layers oxidized at different temperatures that oxygen content increases distinctly up to about 20 at.% at  $900^\circ\text{C}$  and nitrogen content drastically decreases when oxidation is performed at the temperature higher than  $800^\circ\text{C}$ . Moreover, the N content decreases when the annealing is prolonged up to 30 min (Fig. 5).

The diffraction patterns obtained for the TiAlN+IN718 diffusion couple are presented in Fig. 5. Due to the diffusion of oxygen to the TiAlN (200) coating (at around  $2\Theta = 43.8^\circ$ ), a stable  $\text{Al}_2\text{O}_3$  ceramic layer is formed and this fact is documented by two distinct diffraction peaks on X-ray diffraction (XRD) diagram corresponding to two dominant crystallographic orientations (104) and (110) detected at around  $2\Theta = 36^\circ$  and  $38^\circ$  respectively.

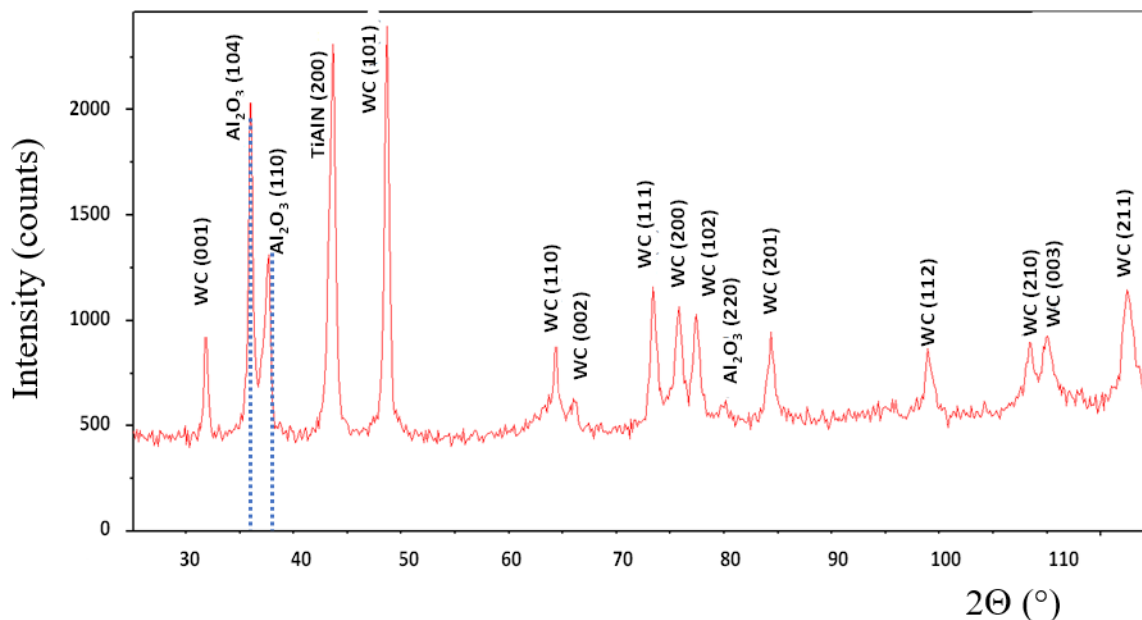


Fig. 6. XRD analysis result of investigated TiAlN+IN718 diffusion couple after oxidation at  $900^\circ\text{C}$  during 10 min

Because a distinct peak for TiAlN (200) is detected at  $2\Theta = 43.8^\circ$  in the XRD spectrum, the TiAlN phase is still present in the partially oxidized layer, which suggests that the oxidation of the surface layer was not yet completed.

#### 4. TOOL WEAR TESTS

In this experimental study the tool wear test represents the dynamic diffusion test performed under thermo-mechanical conditions similar to the special diffusion couple test described in Section 2.2. Figures 7a and 7b present SEM images of worn rake and flank faces after the machining time of 0.5 min and 2.5 min respectively. Similar flank wear in the form of severe notching is also reported in Refs. [7, 10, 15]. The examination of the chemical compositions of wear product in different localizations marked by point numbers was performed based on EDS analysis.

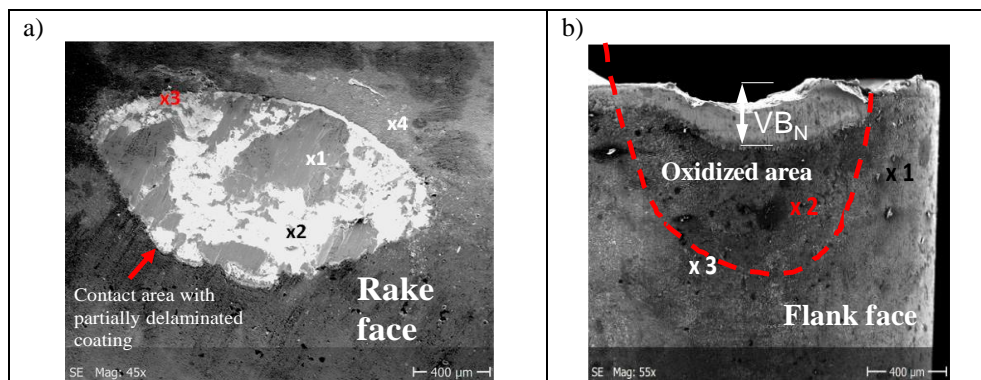


Fig. 7. SEM images of rake (a) and flank (b) faces obtained after machining of IN 718 workpiece with the cutting speed of 200 m/min; the machining time of 0.5 min (a) and 2.5 min (b)

Table 3. EDS analysis results in point #1, #2, #3 and #4 at the rake face marked in Fig. 7a

Place/ Point #	Element (at.%)								
	C	W	Fe	O	Al	N	Ti	Ni	Cr
1	-	-	-	4.8	8.34	4.9	10.89	49.97	21.10
2	17.71	71.3	1.74	-	-	-	0.19	5.65	3.41
3	-	-	-	22.91	19.81	32.87	24.41	-	-
4	-	-	-	-	22.01	48.32	29.67	-	-

It can be noted based on data specified in Table 3 that the SEM image of the worn rake face shown in Fig. 7a includes the following characteristic sub-areas:

- In point #1 IN 718 alloy is smeared on the substrate,
- In point #2 WC-Co substrate is exposed, i.e. the coating is removed,
- In point #3 the oxidized layer is present.
- In point #4 TiAlN coating is detected (only slightly abrasively treated).

Table 4. The estimated chemical compositions of worn area at the flank face measured by EDS

Point number	Element (at%)		
	O	Al	Ti
1	7.92	29.70	63.00
2	17.28	27.54	55.18
3	8.91	26.31	64.78

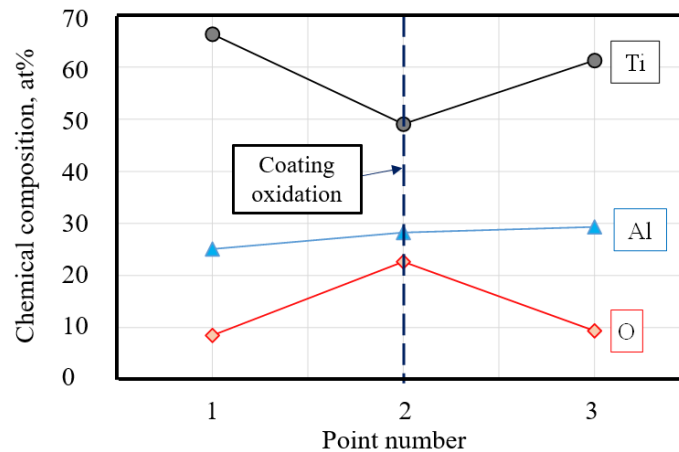


Fig. 8. Chemical compositions detected in points #1, #2 and #3 at the flank faces in Fig. 7b after machining of IN 718 alloy with the cutting speed of 200 m/min; the machining time of 30s (data specified in Table 3)

Table 4 specifies the at.% contents of oxygen (O), aluminium (Al) and titanium (Ti) detected in the oxidized area at the flank face which covers the notch groove. As previously these data are visualized in Fig. 8 showing the chemical composition corresponding to the coating oxidation. It was predicted based on the chemical compositions of oxidized coating in point #2 that the notch wear of about 300  $\mu\text{m}$  was developed after 2.5 min machining trial due to the increase of the oxygen content to about 18at%. It should be noticed that this O content is practically the same as in Table 2 for the diffusion couple (about 17at%).

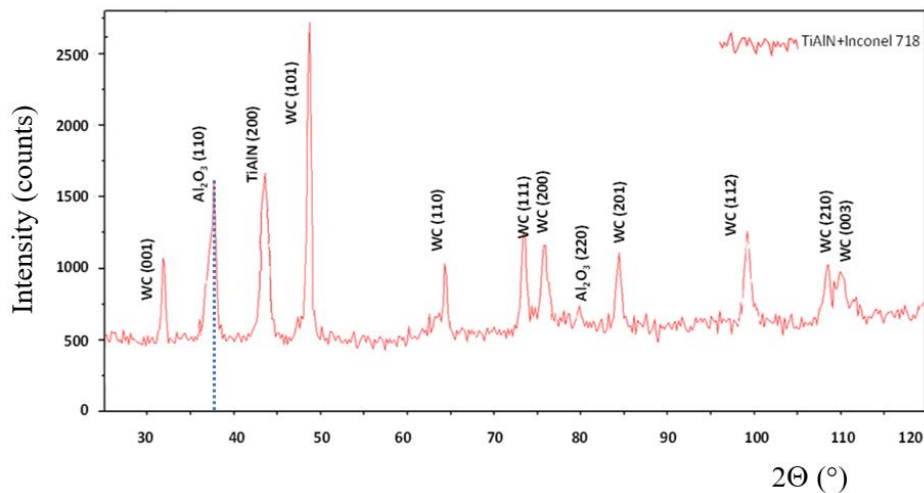


Fig. 9. XRD analysis results of the investigated coating after oxidation during machining tests

The diffraction patterns obtained for the TiAlN coating oxidized in the vicinity of point #2 in Fig. 7b are presented in Fig. 9. Similarly as in the diagram shown in Fig. 6 the TiAlN (200) coating is depicted by a distinct peak at around  $2\Theta = 43.8^\circ$ . In consequence, the formation of a stable  $\text{Al}_2\text{O}_3$  ceramic layer is documented by a distinct diffraction peak on

the X-ray diffraction (XRD) diagram corresponding to the dominant crystallographic orientation (110) detected at around  $2\Theta = 38^\circ$ . This fact can be an argument for the similarity of TiAlN coating oxidization in the diffusion couple (static diffusion test) and during natural tool flank wear (dynamic diffusion test).

## 5. CONCLUSIONS

1. An original methodology for investigating oxidation effects for a TiAlN coating based on special diffusion couple tests under defined temperature regimes is proposed.
2. It was verified, based on EDS and XRD analyses, that the oxidation of TiAlN coatings at the temperature of about  $900^\circ\text{C}$  performing in the static and dynamic diffusion tests results in comparable chemical compositions of the oxidized outer layers.
3. Tool wear tests revealed that oxidation of TiAlN coating deposited on the flank face results in the initiation and evolution of notch wear in the vicinity of the primary cutting edge due to the penetration of ambient atmospheric air.
4. The comparison of XRD patterns showed that  $\text{Al}_2\text{O}_3$  oxide layers produced in static and dynamic diffusion tests have the same crystallographic orientations (104). It is a convincing argument for the fact that the flank face grooving is caused by the intensive oxidation of the cutting tool.

## REFERENCES

- [1] GRZESIK W., 2017, *Advanced Machining Processes of Metallic Materials*, Elsevier, Amsterdam.
- [2] M'SAOUBI R., AXINTE D., SOO S.L., NOBEL CH., ATTIA H., KAPPMAYER G., ENGIN S., SIM W.M., 2015, *High Performance Cutting of Advanced Aerospace Alloys and Composite Materials*, CIRP Annals-Manufacturing Technology, 64/2, 557–580.
- [3] BOUZAKIS K.D., MICHAILIDIS N., SKORDARIS G., BOUZAKIS E., BIERMAN D., M'SAOUBI R., 2012, *Cutting with Coated Tools: Coating Technologies, Characterization Methods and Performance Optimization*, CIRP Annals-Manufacturing Technology, 61/2, 587–609.
- [4] KUTSCHEJ K., MAYRHOFER P.H., KATHREIN M., POLCIK P., TESSADRI R., MITTERER C., 2005, *Structure, Mechanical and Tribological Properties of Sputtered  $\text{Ti}_{1-x}\text{Al}_x\text{N}$  Coatings with  $0.5 \leq x \leq 0.75$* , Surface Coating Technology, 200, 2358–2365.
- [5] NIEŚŁONY P., GRZESIK W., LASKOWSKI P., ŻAK K., 2015, *Numerical 3D FEM Simulation and Experimental Analysis of Tribological Aspects in Turning Inconel 718 Alloy*, Journal of Machine Engineering, 15/1, 47–57.
- [6] KLOCKE F., 2011, *Manufacturing Technology I. Cutting*, Springer, Berlin.
- [7] XAVIOR A., MANOHAR M., JEYAPANDARAJAN P., MADHUKAR P., 2017, *Tool Wear Assessment During Machining of Inconel 718*, Procedia Engineering, 174, 1000–1008.
- [8] GRZESIK W., NIEŚŁONY P., HABRAT W., 2018, *Investigation of Tool Wear in the Turning of Inconel 718 Superalloy in Terms of Process Performance and Productivity Enhancement*, Tribology International, 118, 337–346.
- [9] BUSHLYA V., BJERKE A., TURKEVICH V.Z., LENRICK F., PETRUSHA I.A., CHEREDNICHENKO K.A., STAHL J.E., 2019, *On Chemical and Diffusional Interactions Between PCBN and Superalloy Inconel 718: Imitational Experiments*, Journal of the European Ceramic Society, 39, 2658–2665.

- [10] BUSHLYA V., LENRICK F., STÄHL J.E., M'SAOUBI R., 2018, *Influence of Oxygen on the Tool Wear in Machining*, CIRP Annals-Manufacturing Technology, 67/1, 79–82.
- [11] HATT O., CRAWFORTH P., JACKSON M., 2017, *On the Mechanism of Tool Crater Wear During Titanium Alloy Machining*, Wear, 374–375, 15–20.
- [12] GRECZYNSKI G., HULTMAN L., ODEN M., 2019, *X-Ray Photoelectron Spectroscopy Studies of  $Ti_{1-x}Al_xN$  ( $0 \leq x \leq 0.83$ ) High Temperature Oxidation: The crucial role of Al concentration*, Surface and Coatings Technology, 374, 923–934.
- [13] GRZESIK W., MAŁECKA J., KWAŚNY W., 2020, *Identification of Oxidation Process of TiAlN Coatings Versus Heat Resistant Aerospace Alloys Based on Diffusion Couples and Tool Wear Tests*, CIRP Annals-Manufacturing Technology, 69/1, 41–44.
- [14] GRZESIK W., 2020, *Modelling of Heat Generation and Transfer in Metal Cutting: a Short Review*, Journal of Machine Engineering, 20/1, 24–33.
- [15] CANTERO J.L., DIAZ-ALVAREZ J., MIGUELEZ M.H., MARIN N.C., 2013, *Analysis of Tool Patterns in Finishing Turning of Inconel 718*, Wear, 297, 885–894.